Lawrence Berkeley National Laboratory

Title

Homoleptic versus Heteroleptic Formation of Mononuclear Fe(II) Complexes with Tris-Imine Ligands

Permalink

Journal

ISSN

Authors

Barrios, Leoní A
Bartual-Murgui, Carlos
Peyrecave-Lleixà, Eugènia
et al.

Publication Date

DOI

Peer reviewed

Homoleptic *versus* heteroleptic formation of mononuclear Fe(II) complexes with tris-imine ligands.

Leoní A. Barrios,[†] Carlos Bartual-Murgui, [†,‡] Eugènia Peyrecave-Lleixà,[†] Boris Le Guennic,[§] Simon J. Teat,[‡] Olivier Roubeau,[‡,*] and Guillem Aromí[†,*]

[†] Departament de Química Inorgánica, Universitat de Barcelona, Diagonal 645, 08028, Barcelona-Spain,

[‡] Instituto de Ciencia de Materiales de Aragón, CSIC and Universidad de Zaragoza, Plaza San Francisco s/n, 50009 Zaragoza, Spain,

[§] Institut des Sciences Chimiques de Rennes, UMR 6226 CNRS-Université de Rennes 1, 263 Avenue du Genéral Leclerc, 35042 Rennes Cedex, France,

[‡] Advanced Light Source, Berkeley Laboratory, 1 Cyclotron Road, Berkeley, California 94720.

*KEYWORDS Homoleptic and heteroleptic complexes, Iron (II), tris-imine ligands, spin crossover*

Supporting Information Placeholder

ABSTRACT: We show a marked tendency of Fe(II) to form heteroleptic [Fe(L)(L')](ClO_4)$_2$ complexes from pairs of chelating tris-imine 3bpp, tpy or 2bbp ligands. New synthetic avenues for spin crossover research become thus available, here illustrated with three new heteroleptic compounds with differing magnetic behaviours; [Fe(H$_4$L1)(Cl-tpy)](ClO_4)$_2$·C$_3$H$_6$O (**1**), [Fe(H$_2$L3)(Me3bpp)](ClO_4)$_2$·C$_3$H$_6$O (**2**), [Fe(H$_4$L1)(2bbp)](ClO_4)$_2$·3C$_3$H$_6$O (**3**). Structural studies demonstrate that **1** is in the low spin (LS) state up to 350 K while complexes **2** and **3** are, by contrast, in the high spin (HS) state down to 2 K, as corroborated through magnetic susceptibility measurements. Upon exposure to the atmosphere, the latter exhibits the release of three molecules of acetone per complex, turning into the solvent free analogue [Fe(H$_4$L1)(2bbp)](ClO_4)$_2$ (**3a**), through a single-crystal-to-single-crystal transformation. This guest extrusion process is accompanied by a spin switch, from HS to LS.

Introduction

Spin crossover (SCO) compounds are among the currently most promising switchable molecular materials.[1] The renewed interest in this phenomenon due to its potential in the fabrication of functional nano-devices[2-4] has fuelled fundamental research to understand it and exploit it conveniently. A crucial question is the intimate relationship between the chemical interactions that propagate throughout the crystal lattice and the dynamics of the transition.[5,6] These interactions govern the occurrence or absence of bistability, a consequence of the cooperativity within the material.[7] With such an aim, the contribution of synthetic chemistry is paramount, since it allows designing and tuning the intermolecular interactions within a crystallographic network. In this context, the chelating ligands of the type 2,6-bis(pyrazol-*x*-yl)pyridine (*x* = 1 or 3, *ie* 1bpp or 3bpp) are very attractive, since they generate the appropriate ligand field to observe SCO of Fe(II) and lead to complexes with a dense network of intermolecular interactions.[8,9] We have produced a family of 3-bpp ligands (H$_4$L1, H$_2$L2 or H$_2$L3 in Fig. 1) designed to augment the amount of π···π, C–H···π and/or H–bonding interactions,[8,10-12] and used them to study the dynamics of the HS→LS relaxation of metastable states.[13] We recently discovered that mixing two different 3bpp ligands of varying length (3bpp and H$_2$L2, Fig. 1) led to the quantitative crystallization of the heteroleptic complex [Fe(H$_2$L2)(3bpp)](ClO_4)$_2$·*solvents*, which exhibits remarkable reversible solvent molecule exchange dynamics.[14,15]
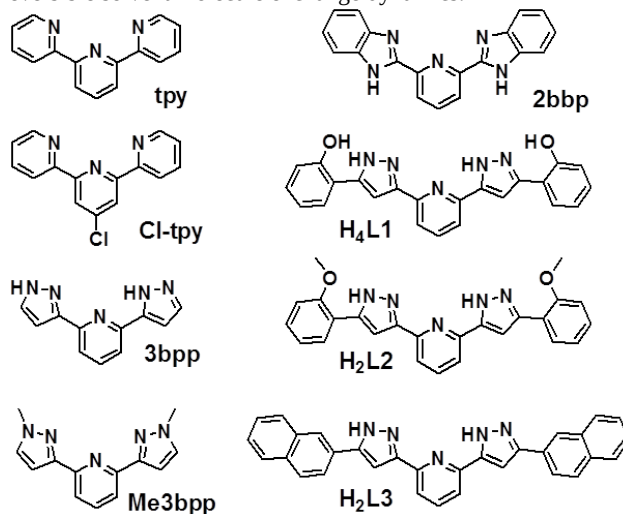
Figure 1. Ligands employed in this work. tpy, 2,6-bis-(pyridine-2-yl)-pyridine; Cl-tpy, 2,6-bis-(pyridine-2-yl)-4-chloro-pyridine; 3bpp, 2,6-bis(pyrazol-3-yl)-pyridine; Me3bpp, 2,6-bis(1-methylpyrazol-3-yl)-pyridine; 2bbp, 2,6-bis(2-benzimidazolyl)-pyridine; H$_4$L1, 2,6-bis(5-(2-hydroxyphenyl)-pyrazol-3-yl)-pyridine; H$_2$L2, 2,6-bis(5-(2-methoxyphenyl)-pyrazol-3-yl)-pyridine and H$_2$L3, 2,6-bis(5-naphthyl-pyrazol-3-yl)-pyridine.

This suggests that the potential of forming heteroleptic analogues could increase exponentially the options of preparing and studying novel SCO complexes. We have thus engaged on a study to specifically verify if this reactivity can be generalized and to gather the reasons for the formation of hetero- or homoleptic complexes. We expanded this investigation to tridentate ligands of the 2,6-bis(pyridin-2-yl)pyridine (tpy, Fig. 1) and of the 2,6- bis(benzimidazol-2-yl)pyridine (2bbp, Fig. 1) types, which have produced Fe(II) SCO complexes before.[16-20]

Experimental

Synthesis

Ligands H$_4$L1, H$_2$L2 and H$_2$L3 were prepared according to procedures previously reported by us.[10-12] CAUTION: Perchlorate salts of metal complexes are potentially explosive. Only small quantities of material should be prepared and the samples should be handled with care.

[Fe(H$_4$L1)(Cl-Tpy)](ClO$_4$)$_2$·C$_3$H$_6$O (1). A suspension of H$_4$L1 (0.012 g, 0.03 mmol) and Cl-Tpy (0.007 g, 0.03 mmol) in acetone (5 mL) was added dropwise to a stirred solution of Fe(ClO$_4$)$_2$·6H$_2$O (0.025 g, 0.07 mmol) and ascorbic acid (~3 mg) in acetone (5 mL). The resulting dark orange solution was stirred for 40 min at room temperature, before being layered with diethyl ether (volume 1:1). Crystals formed after 3 days (0.004 g, 13%). EA, calcd (%) for C$_{41}$H$_{35}$Cl$_3$FeN$_8$O$_{12}$, **1**·H$_2$O (found): C, 49.54 (49.83); H, 3.55 (3.41); N, 11.27 (11.29).

[Fe(H$_2$L3)(Me3bpp)](ClO$_4$)$_2$·C$_3$H$_6$O (2). A suspension of H$_2$L3 (0.026 g, 0.056 mmol) and Me3bpp (0.013 g, 0.056 mmol) in acetone (10 mL) was added dropwise to a stirred solution of Fe(ClO$_4$)$_2$·6H$_2$O (0.045 g, 0.123 mmol) and ascorbic acid (~3 mg) in acetone (10 mL). The resulting orange solution was stirred for 45 min at room temperature, before being filtered and layered with toluene (volume 1:1). Crystals formed after 7 days (19,2 mg, 36%). EA, calcd (%) for C$_{47}$H$_{40}$Cl$_2$FeN$_{10}$O$_9$, **2** (found): C, 55.61 (55.88); H, 3.97 (3.92); N, 13.81 (13.72).

[Fe(H$_4$L1)(2bbp)](ClO$_4$)$_2$ (3a). A suspension of H$_4$L1 (0.012 g, 0.03 mmol) and 2bbp (0.009 g, 0.03 mmol) in acetone (5 mL) was added dropwise to a stirred solution of Fe(ClO$_4$)$_2$·6H$_2$O (0.025 g, 0.07 mmol) and ascorbic acid (~3 mg) in acetone (5 mL). The resulting dark orange solution was stirred for 40 min at room temperature, before being layered with diethyl ether (volume 1:1). Crystals formed after 4 days. The crystals were filtered and dried in air, changing colors rapidly from orange to very dark. EA, calcd (%) for C$_{42}$H$_{34}$Cl$_2$FeN$_{10}$O$_{12}$, **3a**·2H$_2$O (found): C, 50.57 (50.35); H, 3.44 (3.05); N, 14.04 (13.82).

[Fe(tpy)$_2$](ClO$_4$)$_2$·H$_2$O (5). A suspension of H$_4$L1 (0.012 g, 0.03 mmol) and Tpy (0.006 g, 0.03 mmol) in acetone (5 mL) was added dropwise to a stirred solution of Fe(ClO$_4$)$_2$·6H$_2$O (0.025 g, 0.07 mmol) and ascorbic acid (~3 mg) in acetone (5 mL). The resulting dark orange solution was stirred for 40 min at room temperature, before being layered with diethyl-ether (volume 1:1). Crystals formed after 3 days (0.007 g, 32%). EA, calcd (%) for C$_{30}$H$_{23}$Cl$_2$FeN$_6$O$_{8.5}$, **5**–0.5H$_2$O (found): C, 49.38 (49.20); H, 3.18 (2.94); N, 11.52 (11.44).

Physical Measurements

The elemental analysis was performed with an Elemental Microanalizer (A5), model Flash 1112 at the Servei de Microanàlisi of CSIC, Barcelona, Spain. IR spectra were recorded as KBr pellet samples on a Nicolet AVATAR 330 FTIR spectrometer. MALDI-TOF mass spectrometry measurements were performed on performed on a 400 ABSciex MALDI-TOF spectrometer at the Unitat d'Espectrometria de Masses de Caracterització Molecular (CCiT) of the University of Barcelona. Samples were prepared as follows; 5 ☐l of the solution were diluted in 5 ml of MeOH. Then, 0.5☐l of internal reference solution, containing 10 mg/ml of DCTB in dichloromethane were added before injection. Magnetic measurements were performed on polycrystalline samples in a 0.5 T *dc* applied field with a MPMS-XL magnetometer at the Physical Measurements Service of the Servicio de Apoyo a la Investigación-SAI, Universidad de Zaragoza. Diamagnetic corrections for the sample holder, determined empirically, and for the sample diamagnetic contribution were applied. Measurements on compound **3** were restricted to $T < 200$ K after inserting the crystals directly at 200 K and purging the sample space at this temperature, to avoid the easy transformation suffered by the crystals upon loss of lattice acetone.

X-ray crystallography.

Experimental details are provided in the supplementary material. Crystallographic and refinement parameters are summarized in Table S1. Selected bond lengths and angles are given in Tables 1 and S2.

All details can be found in CCDC 1052140 and 1052142 (**1**-100 K and **5**), CCDC 1453126 (**2**), CCDC 1403617-1403618 (**3**, **3dis** and **3a**) and 1052608 (**1**-350 K) that contain the supplementary crystallographic data for this paper. These data can be obtained free of charge from The Cambridge Crystallographic Data Centre via www.ccdc.cam.ac.uk/data_request/cif.

Computational details

DFT geometry optimizations were carried out by using the Gaussian 09 (revision D.01) package[21] with the PBE0 hybrid functional,[22,23] and tightening both self-consistent field (10^{-10} au) and geometry optimization (10^{-5} au) convergence thresholds. The "Stuttgart/Dresden" basis sets and effective core potentials were used to describe the iron atom,[24] whereas all other atoms were described with the SVP basis sets.[25] In all steps, a modelling of bulk solvent (acetone and methanol) effects was also included through the polarizable continuum model (PCM).[26]

The preference in ligand distribution around Fe(II) for a given

L1/L2 ligand combination was gauged by the sign of the energy difference $\Delta E = 2E([Fe(L1)(L2)]^{2+}) - E([Fe(L1)_2]^{2+}) - E([Fe(L2)_2]^{2+})$.

Results and discussion

Synthesis

The reaction in acetone of $Fe(ClO_4)_2$ with five different equimolar mixtures of two ligands produced, upon layering with Et_2O or toluene (SI), crystals of the heteroleptic compounds $[Fe(H_4L1)(Cl\text{-tpy})](ClO_4)_2 \cdot C_3H_6O$ (1), $[Fe(H_2L3)(Me3bpp)](ClO_4)_2 \cdot C_3H_6O$ (2), $[Fe(H_4L1)(2bbp)](ClO_4)_2 \cdot 3C_3H_6O$ (3), $[Fe(H_2L2)(3bpp)](ClO_4)_2 \cdot 1.5C_3H_6O$ (4)[14] and the homoleptic system $[Fe(tpy)_2](ClO_4)_2 \cdot H_2O$ (5) for combinations Cl-tpy/H$_4$L1,[27] Me3bpp/H$_2$L3,[10] 2bbp/H$_4$L1, 3bpp/H$_2$L2 (previously reported by us)[14] and tpy/H$_4$L1, respectively (see Fig. 1 and caption for ligand structures and names). The molecular structure of all compounds was determined by single crystal X-ray diffraction. Thus, of the five combinations, four produced crystals of pure heteroleptic assemblies in reasonable yield whereas one led to the sole crystallization of one of the homoleptic derivatives. To the best of our knowledge, there are no precedents in the literature of heteroleptic Fe(II) complexes with two different ligands of the tris-imine kind, with the exceptions of compound 2[14] and complex $[Fe(H_4L1)(H_2L1a)]BF_4$, also reported by our group.[28] The latter was obtained accidentally after the partial *in situ* fluoroboration of H$_4$L1 into H$_2$L1a, which then participates of the reaction. The potential of generating a large new family of heteroleptic complexes is very promising, since the combination of ligands with different properties allows to see manifestations of SCO that otherwise would not be observed.[29] A polymorph of the homoleptic species 5 had been reported long-time ago, as obtained by crystallization in water.[30] Its room temperature parameters (especially the Fe–N distances) showed it to be LS. The structure of 5 (SI) also shows it to be LS at 100 K. The structure of 4 has been recently reported by us and it is LS over the whole range of temperatures before it experiences a single-crystal-to-single-crystal (SCSC) transformation (near 320 K) to turn into a new solvate in the HS state.[14,15]

Description of the Structures

Compounds 1, 2 and 3 are reported here for the first time and their structure is described below (see also Tables 1, S1 and S2).

[Fe(H$_4$L1)(Cl-Tpy)](ClO$_4$)$_2$·C$_3$H$_6$O (1). Complex 1 crystallizes in the $P2_1$ space group. The unit cell contains a full $[Fe(H_4L1)(Cl\text{-tpy})]^{2+}$ heteroleptic complex cation, two ClO_4^- anions compensating the positive charge and one molecule of acetone. Two such units are incorporated into the unit cell. The complex features an Fe(II) center coordinated to both mutually perpendicular tridentate ligands (Fig. 2). Ligand H$_4$L1 exhibits two intramolecular hydrogen bonds, resulting from the orientation of both hydroxophenyl groups towards the center of the molecule (*syn,syn*). The Fe–N distances at 100 K (average, 1.961 Å) indicate the metal to be in the LS state. The acetone molecule and one ClO_4^- anion form strong H-bonds with the O–H and/or the N–H groups of the complex (Fig. S1, Table S2). The second anion is located in a hydrophobic cavity and only exhibits weaker O···H–C interactions. The cations are organized in sheets exhibiting an unconventional form of the

"terpy embrace"[28] where each species is surrounded by six first neighbours (instead of four) establishing a total of six π···π interactions of varying intensity and eight C–H··· π contacts (Fig. S2). Within the layers, these units are organized as infinite chains with two alternating different orientations (angle between equatorial planes, 59.32°) that pivot around infinite stacks of phenolic rings, acting as hinges (Fig. 3).

The structure of 1 was also determined at 350 K (Tables 1, S1 and S2). All features are essentially identical to those at 100 K, including the spin state, which remains LS at this temperature.

[Fe(H$_2$L3)(Me$_3$bpp)](ClO$_4$)$_2$·C$_3$H$_6$O (2). The space group of 2 is $P2_1$ while the content of its asymmetric unit corresponds to its empirical formula (Fig. S3). The Fe(II) center of the complex at 100 K is in the HS state (average Fe–N dist. of 2.164 Å) and features two different tridentate ligands disposed opposite to each other forming a "cross" (Fig. 2). The cations of 3 also organize as sheets, with each complex surrounded by six first neighbours through six π···π bonds and three C–H···π interactions (Fig. S4). The species in these layers have all the same orientation and exhibit also infinite stacks of well aligned distal aromatic rings (Fig. S5). Magnetic susceptibility measurements show that compound 2 maintains its HS state down to 2K (Fig. S6).
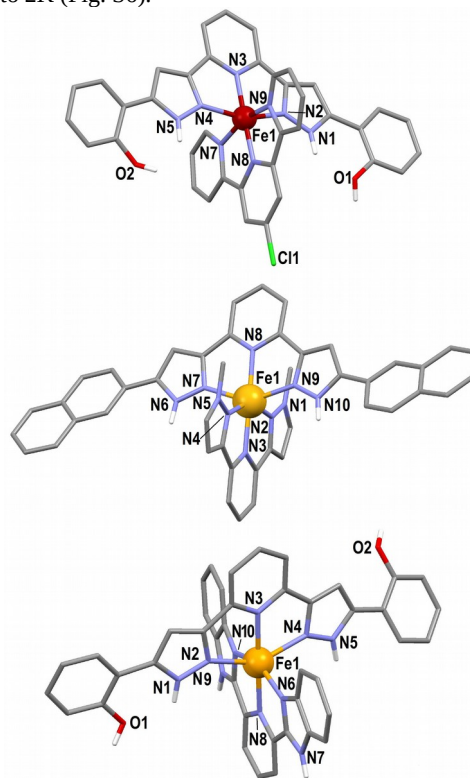
Figure 2. Structure of the complex cations within compounds $[Fe(H_4L1)(Cl\text{-tpy})](ClO_4)_2 \cdot C_3H_6O$ (1, top), $[Fe(H_2L3)(Me3bpp)](ClO_4)_2 \cdot C_3H_6O$ (2, middle) and $[Fe(H_4L1)(2bbp)](ClO_4)_2 \cdot 3C_3H_6O$ (3, bottom), with heteroatoms labelled. Only hydrogen atoms bound to heteroatoms shown. Carbon and hydrogen atoms are in grey and white respectively. LS and HS Fe(II) are in red and yellow, respectively.
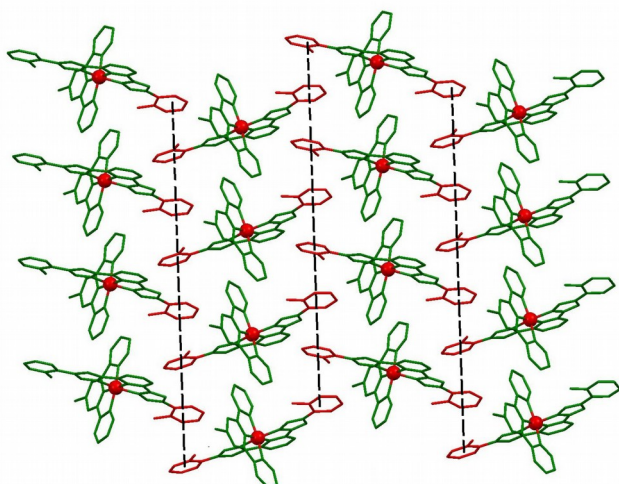
Figure 3. Molecular representation of the sheets of the [Fe(H₄L1)(Cl-tpy)]²⁺ cations in **1** emphasizing the stripes of phenol groups (red) running throughout the sheets, connected by a series of π···π contacts (dashed lines).

Table 1. Selected bond distances (Å) in the structures of compounds **1**, **2**, **3**, **3a** and **5**.

	1		**2**		**3**	
	(100 K)	(350 K)				
Fe1–N8	1.885(11)	1.879(7)	Fe1–N3	2.110(5)	Fe1–N3	2.1295(14)
Fe1–N3	1.927(11)	1.921(7)	Fe1–N8	2.138(5)	Fe1–N8	2.1310(15)
Fe1–N7	1.969(11)	1.979(7)	Fe1–N9	2.160(5)	Fe1–N6	2.1533(15)
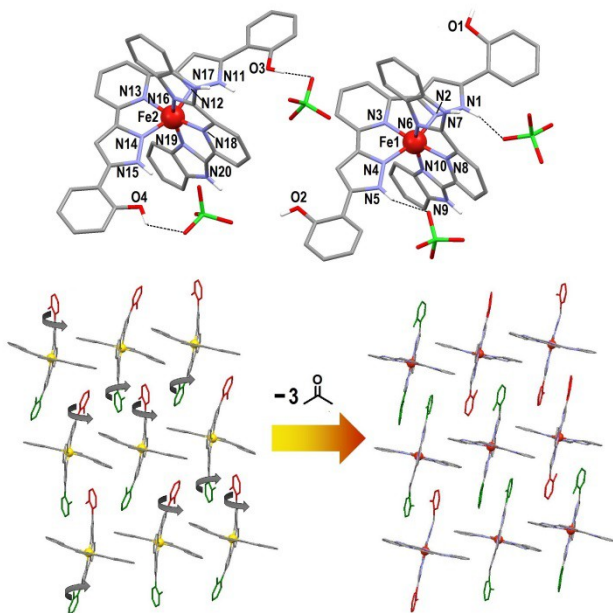
[Fe(H₄L1)(2bbp)](ClO₄)₂·3C₃H₆O (3). Compound **3** crystallizes in the *P*–1 group, its asymmetric unit coinciding with the formula unit. Of this formula, the central [Fe(H₄L1)(2bbp)]²⁺ cation is linked to two ClO₄⁻ and three acetone species through hydrogen bonds with N–H or O–H groups from the ligands (Fig. S7). At 100 K, the complex is already in its HS state (average Fe–N dist. of 2.164 Å). Magnetic susceptibility measurements confirm that this state is maintained down to 2K (Fig. S6). The ligand H₄L1 features now the *anti*,*syn* conformation (Fig. 2), different from that seen

in **1**. The cations are organized as sheets in a modified version of the "terpy embrace", featuring five first neighbors connected through π···π and C–H··· π interactions (Fig. S8). Here the distal phenol groups of H₄L1 establish intermolecular stacks in groups of four (Fig. S9).

Figure 4. (top) Asymmetric unit of [Fe(H₄L1)(2bbp)](ClO₄)₂ (**3a**), from desolvation of **3**, with heteroatoms labelled. Only hydrogen atoms bound to heteroatoms shown. Carbon and hydrogen atoms are in grey and white respectively. Hydrogen bonds involving ClO₄⁻ shown. (bottom) Representation of the cations in **3** -*left*- and **3a** -right-, emphasizing the rotation by 180° of 50% of the distal phenol groups of H₄L1 in passing from one to the other. Green and red represent the two orientations of these groups with respect to the plane of the sheet.

Very interestingly, the orange crystals of **3** turn almost black after a few minutes of exposure to the atmosphere, experiencing some degradation. Nevertheless, the new system, **3a**, could be analysed by single crystal X-ray diffraction. The experiment revealed that as soon as the crystals of **3** are extracted from their mother liquor, the material releases all the lattice acetone molecules (Fig. 4).

This causes drastic changes to the structure and a magnetic transition. Thus, **3a** is found in the *P*–1 space group, while the asymmetric unit contains now two inequivalent [Fe(H₄L1)(2bbp)](ClO₄)₂ ensembles with no solvents. The perchlorates are all hydrogen bonded to N–H groups (Table S2), and in both inequivalent complexes, the H₄L1 ligand has changed conformations, now being either *syn,syn* or *anti,anti* (Fig. 4).

The larger packing efficiency of the complexes upon solvent release may be gauged by the reduction of the lattice volume taking place, which amounts to a 23% contraction (SI). The process also involves a transition to the LS state (average Fe–N distances in **3a**; 1.925 and 1.918 Å), which may contribute to the shrinkage. Magnetic susceptibility measurements confirm that this state is maintained up to 300K (Fig. S6). The analysis of the dessolvated product shows the presence of two equivalents of H₂O over time, very likely resulting from water absorption by the "empty" network from the atmosphere over time. However, the bulk magnetization measurements were performed short after the compound was exposed to the atmosphere, thus likely corresponding to **3a**. Most surprisingly about the solvent extrusion process, the migration of acetone takes place through a rotation of nearly 180° by 50% of the PhOH rings of the H₄L1 ligands (Fig. 4). This rotation certainly facilitates the diffusion of guest molecules through the compact lattice, as in a revolving door,[31] with persistence of the ordered crystal lattice. The latter is presumably facilitated by the better organization of the complexes in the solid state, each interacting with more and better contacts through and "expanded" terpy embrace (four first neighbours plus two second neighbours also establishing intermolecular interactions; Figs. 5 and S10). We recently reported a similar process of ordered acetone extrusion accompanied by a SCO and a first order crystallographic transition in **4**, and demonstrated that it takes place through a fully ordered solid state intermediate.[15] It will be interesting to investigate also the **3 → 3a** transformation to elucidate the mechanism of this intricate solid state reaction.
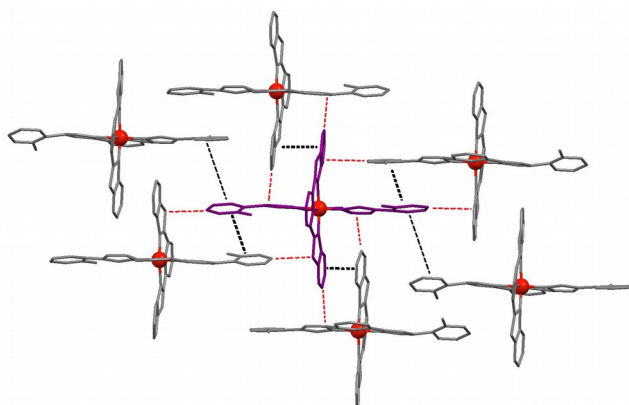
Figure 5. Representation of the supramolecular sheets of [Fe(H₄L1)(2bbp)]²⁺ cations in **3a**, emphasizing the six π···π interactions (black dashed lines, two weaker than the others) and eight C–H···π interactions (red dashed lines) between each cation and its four first neighbours and two second neighbours.

Mass Spectrometry

With the aim to investigate the formation in solution of either heteroleptic or homoleptic derivates for each combination of ligands, mass spectrometry was used. Thus, positive MALDI-
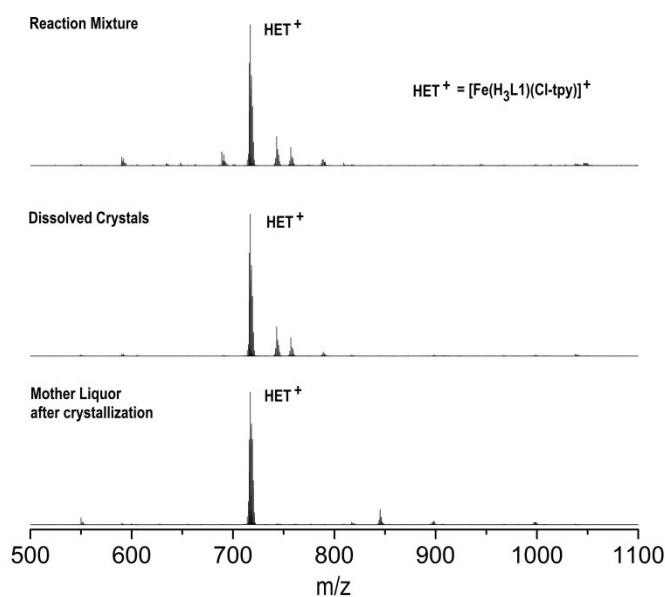
TOF mass spectrometry (MS) diagrams for each system were determined for the original reaction mixture, for the remaining mother liquor after the conclusion of the crystallization and from solutions of the isolated crystals, always using acetone as solvent, while methanol was employed to dilute the samples before injection. It must be kept in mind however, that MS is not a quantitative technique, thus, the information obtained from these experiments must be considered as a qualitative guide. Full data for these can be found in the SI. The MS of the reaction mixture for the Cl-tpy/H₄L1 combination is clearly dominated by a peak of the heteroleptic species; the cation of **1** (Fig. 6). After crystallization of **1**, the MS of the solution still shows only the heteroleptic entity, as does that of the isolated product dissolved in acetone. This indicates that the heteroleptic species is preferred over the homoleptic ones. The

fact that the former is the only one that crystallizes is consistent with this and with its favorable organization in a crystal lattice.

Figure 6. MALDI-TOF MS diagrams of the reaction of the combination Cl-tpy/H₄L1 with Fe(ClO₄)₂ upon mixing of the reagents, after isolating the crystals and dissolving them and of the mother liquor after separating the crystals.

A similar behavior was observed for the reaction with Me3bpp/H₂L3 (Fig. S11), although less marked; the heteroleptic species is the only one isolated (**2**) and the solution also shows some preference for it, although with the minor presence of some homoleptic combination. Interestingly, the combination 3bpp/H₂L2 exhibits a completely different behaviour; all the reaction mixtures show a clear dominance of the homoleptic species (Fig. S12) whereas the isolated product is again the heteroleptic complex **4**. Therefore, the energy of complexation would explain the overruling presence of peaks from [Fe(3bpp)₂]²⁺ and [Fe(H₂L2)₂]²⁺ in solution while the packing efficiency of [Fe(H₂L2)(3bpp)](ClO₄)₂ leads to its segregation in the solid state. This is nicely confirmed upon redissolution of **4**, which restores the original distribution with a preference of the homoleptic species again, following the disproportionation of [Fe(H₂L2)(3bpp)]²⁺. The behavior of the 2bpp/H₄L1 reaction system is somewhere in between the above two patterns. Thus, while the solutions always display comparable amounts the heteroleptic and homoleptic analogues, the crystallized species is always the pure mixed ligand complex [Fe(H₄L1)(2bbp)](ClO₄)₂·3C₃H₆O (**3**). The latter indeed disproportionates to a significant extent when it is brought back to solution, leading to important amounts of homoleptic moieties together with the heteroleptic species (Fig. S13).

Finally, the behavior of the tpy/H₄L1 mixture is again different to that of the previous ones. This system shows a predominant peak of the mixed ligand complex at the initial stage and also in the solution after the separation of the crystals (Fig. S14). Surprisingly however, the pure crystallized product is the homoleptic complex **5**, which indicates that the formation of the heteroleptic species is perhaps favored in solution but not in the solid state. Therefore, the complex formation energy facilitates the presence of the heteroleptic complex only in solution, whereas the stability of the lattice drives the exclusive crystallization of [Fe(tpy)₂](ClO₄)₂ (**5**). This is consistent with the notable presence of [Fe(H₄L1)₂]²⁺ in the mother liquor, after the separation of **5**, which had not been detected originally (Fig. S14). From the above results, heteroleptic associations seem favoured in solution for combinations Cl-tpy/H₄L1, Me₃bpp/H₂L3 and tpy/H₄L1 while for 3bpp/H₂L2 the homoleptic distribution is preferred. However, the stability of the crystal lattice inverts the nature of the isolated product for the last two combinations, which are [Fe(tpy)₂](ClO₄)₂·H₂O (**5**) and [Fe(H₂L2)(3bpp)](ClO₄)₂·1.5 C₃H₆O (**4**), respectively. The undefined tendency in solution for 2bpp/H₄L1 is also fully resolved in the solid state in favor of the heteroleptic arrangement in [Fe(H₄L1)(2bbp)](ClO₄)₂·2C₃H₆O (**3**). In summary, the solid state, as a means to isolate the various products, favors heteroleptic arrangements in four cases out of five.

DFT Calculations

In order to support the experimental observations, DFT calculations were performed (see computational details). The preference in ligand distribution around the Fe(II) ion for a given L1/L2 ligand combination was gauged by the sign of the energy difference $\Delta E = 2E([\text{Fe(L1)}(\text{L2})]^{2+}) - E([\text{Fe(L1)}_2]^{2+}) - E([\text{Fe(L2)}_2]^{2+})$. The absolute electronic energy of each complex cation was calculated on its optimized nuclear configuration obtained both in the HS and LS states taking into account solvent effects through the use of a polarizable continuum model. This configuration is assumed to be the closest possible to the real one for every studied system in solution. The energetically preferred species in solution suggested by the results from MS (see above) are maintained in both spin states (Table S3). Thus, the case where a tendency in solution was most ambiguous (2bpp/H$_4$L1) is predicted to lead slightly to homoleptic species. The same tendency is computed, now more markedly, for the other calculated homoleptic case (3bpp/H$_2$L2), whereas for the rest of the compounds, the DFT results indicate a preference for the heteroleptic combination.

In order to assess any solvent effects, all the above described reactions were performed in several different solvents (methanol, ethanol, acetonitrile, ethylacetate and toluene) and the mass spectra of the corresponding reaction mixtures that did not lead to immediate precipitates were performed using the same respective solvents as a diluting agent. In four cases, the results were consistent with those observed originally (Figs. S15 to S18), confirming the preferred ligand distribution regardless of the solvent. This serves to confirm the validity of the DFT calculations performed to corroborate these observations. The only case where more variability could be observed (Fig. S19) is again the 2bpp/H$_4$L1 system, confirming its undefined behavior in solution.

CONCLUSIONS

In summary, the preparation of three new heteroleptic [Fe(L)(L')](ClO$_4$)$_2$ complexes in addition to one previously reported, with bpp, tpy or bbp ligands confirms a clear tendency for the formation of the mixed ligand species over the homoleptic ones, which opens a vast playground of synthesis for complexes of signified relevance in SCO research. Here great versatility is seen in this respect, one of the heteroleptic complexes is LS (**1**), another is HS (**2**), one is LS and turns HS upon a SCSC transformation following partial extrusion of acetone (**4**) whereas another one, discovered here (**3**), is synthesized as HS and loses three molecules of acetone maintaining crystallinity to turn LS. The preferred distribution in solution not always coincides with the favored product in the solid state, which in the end is the one actually isolated. Most of the times, the latter is the heteroleptic derivative. In order to understand the reasons for either distribution of ligands in the solid state or in solution, it would be of great interest to perform detailed *ab initio* calculations. This, added to more systematic experimental studies would perhaps open the door for exploiting the full potential of the synthetic methodology proposed here.

Supporting Information

This material is available free of charge via the Internet at http://pubs.acs.org.

AUTHOR INFORMATION

Corresponding Authors
*G.A. Tel: +34-934039760. E-mail: guillem.aromi@qi.ub.es
*O.R. Tel: +34976762461. E-mail: roubeau@unizar.es.

ACKNOWLEDGMENT

REFERENCES

(1) Gütlich, P.; Goodwin, H. A. In *Spin Crossover in Transition Metal Compounds I*; Springer-Verlag Berlin: Berlin, 2004; Vol. 233, p 1-47.

(2) Bousseksou, A.; Molnar, G.; Salmon, L.; Nicolazzi, W. *Chem. Soc. Rev.* **2011**, *40*, 3313-3335.

(3) Gamez, P.; Costa, J. S.; Quesada, M.; Aromi, G. *Dalton Trans.* **2009**, 7845-7853.

(4) Gentili, D.; Demitri, N.; Schafer, B.; Liscio, F.; Bergenti, I.; Ruani, G.; Ruben, M.; Cavallini, M. *J. Mater. Chem. C* **2015**, DOI: 10.1039/c1035tc00845j.

(5) Guionneau, P. *Dalton Trans.* **2014**, *43*, 382-393.

(6) Halcrow, M. A. *Chem. Soc. Rev.* **2011**, *40*, 4119-4142.

(7) Halcrow, M. A. *Chem. Lett.* **2014**, *43*, 1178-1188.

(8) Craig, G. A.; Roubeau, O.; Aromi, G. *Coord. Chem. Rev.* **2014**, *269*, 13-31.

(9) Halcrow, M. A. *Coord. Chem. Rev.* **2009**, *253*, 2493-2514.

(10) Barrios, L. A.; Peyrecave-Lleixa, E.; Craig, G. A.; Roubeau, O.; Teat, S. J.; Aromi, G. *Eur. J. Inorg. Chem.* **2014**, 6013-6021.

(11) Craig, G. A.; Costa , J. S.; Aromí, G.; Roubeau, O.; Teat, S. J. *Transactions ACA* **2013**, *44*, 69-85.

(12) Craig, G. A.; Costa, J. S.; Roubeau, O.; Teat, S. J.; Aromi, G. *Chem.-Eur J.* **2011**, *17*, 3120-3127.

(13) Craig, G. A.; Sanchez Costa, J.; Teat, S. J.; Roubeau, O.; Yufit, D. S.; Howard, J. A. K.; Aromi, G. *Inorg. Chem.* **2013**, *52*, 7203-7209.

(14) Sanchez Costa, J.; Rodriguez-Jimenez, S.; Craig, G. A.; Barth, B.; Beavers, C. M.; Teat, S. J.; Aromi, G. *J. Am. Chem. Soc.* **2014**, *136*, 3869-3874.

(15) Aromi, G.; Beavers, C. M.; Sanchez Costa, J.; Craig, G. A.; Minguez Espallargas, G.; Orera, A.; Roubeau, O. *Chem. Sci.* **2016**, DOI:10.1039/C1035SC04287A.

(16) Goodwin, H. A. *Spin Crossover in Transition Metal Compounds I* **2004**, *233*, 59-90.

(17) Linert, W.; Konecny, M.; Renz, F. *J. Chem. Soc., Dalton Trans.* **1994**, 1523-1531.

(18) Boča, R.; Baran, P.; Boča, M.; Dlháň, L. u.; Fuess, H.; Haase, W.; Linert, W.; Papánkova´, B. e.; Werner, R. *Inorg. Chim. Acta* **1998**, *278*, 190-196.

(19) Boča, R.; Baran, P.; Dlháň, L. u.; Fuess, H.; Haase, W.; Renz, F.; Linert, W.; Svoboda, I.; Werner, R. *Inorg. Chim. Acta* **1997**, *260*, 129-136.

(20) Boča, R.; Renz, F.; Boča, M.; Fuess, H.; Haase, W.; Kickelbick, G.; Linert, W.; Vrbová-Schikora, M. *Inorg. Chem. Commun.* **2005**, *8*, 227-230.

(21) M. J. Frisch, G. W. T., H. B. Schle- gel, G. E. Scuseria, M. A. Robb, J. R. Cheeseman, G. Scalmani, V. Barone, B. Mennucci, G. A. Petersson, H. Nakatsuji, M. Caricato, X. Li, H. P. Hratchian, A. F. Izmaylov, J. Bloino, G. Zheng, J. L. Son- nenberg, M. Hada, M. Ehara, K. Toyota, R. Fukuda, J. Hasegawa, M. Ishida, T. Nakajima, Y. Honda, O. Kitao, H. Nakai, T. Vreven, J. A., Jr., Montgomery, J. E. Peralta, F. Ogliaro, M. Bearpark, J. J. Heyd, E. Brothers, K. N. Kudin, V. N. Staroverov, R. Kobayashi, J. Normand, K. Raghavachari, A. Rendell, J. C. Burant, S. S. Iyengar, J. Tomasi, M. Cossi, N. Rega, J. M. Millam, M. Klene, J. E. Knox, J. B. Cross, V. Bakken, C. Adamo, J. Jaramillo, R. Gomperts, R. E. Stratmann, O. Yazyev, A. J. Austin, R. Cammi, C. Pomelli, J. W. Ochterski, R. L. Martin, K. Morokuma, V. G. Zakrzewski, G. A. Voth, P. Salvador, J. J. Dannenberg, S. Dapprich, A. D. Daniels, O. Farkas, J. B. Foresman, J. V. Ortiz, J. Cioslowski, D. J. Fox, Gaussian 09, Revision D.01, 2009, Gaussian Inc, Wallingford, CT.

(22) Perdew, J. P.; Burke, K.; Ernzerhof, M. *Phys. Rev. Lett.* **1996**, *77*, 3865.

(23) Adamo, C.; Barone, V. *J. Chem. Phys.* **1999**, *110*, 6158.

(24) M. Dolg; U. Wedig; H. Stoll; H. Preuss *J. Chem. Phys.* **1987**, *86*, 866-872.

(25) Weigend, F.; Ahlrichs, R. *Phys. Chem. Chem. Phys.* **2005**, *7*, 3297–3305.

(26) Tomasi, J.; Mennucci, B.; Cammi, R. *Chem. Rev.* **2005**, *105*, 2999−3094.

(27) Craig, G. A.; Barrios, L. A.; Costa, J. S.; Roubeau, O.; Ruiz, E.; Teat, S. J.; Wilson, C. C.; Thomas, L.; Aromí, G. *Dalton Trans.* **2010**, *39*, 4874-4881.

(28) Craig, G. A.; Sanchez Costa, J.; Roubeau, O.; Teat, S. J.; Aromi, G. *Chem., Eur. J.* **2012**, *18*, 11703-11715.

(29) Naggert, H.; Rudnik, J.; Kipgen, L.; Bernien, M.; Nickel, F.; Arruda, L. M.; Kuch, W.; Nather, C.; Tuczek, F. *J. Mater. Chem. C* **2015**, DOI: 10.1039/C1035TC00930H.

(30) Baker, A.; Goodwin, H. *Aust. J. Chem.* **1985**, *38*, 207-214.

(31) Coronado, E.; Giménez-Marqués, M.; Mínguez Espallargas, G.; Rey, F.; Vitórica-Yrezábal, I. J. *J. Am. Chem. Soc.* **2013**, *135*, 15986-15989.

For Table of Contents Only
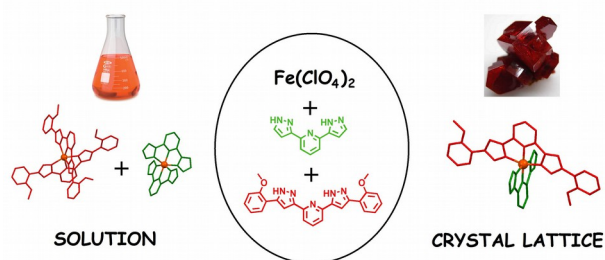
A heteroleptic [Fe(L1)(L2)]$^{2+}$ distribution is the preferred isolated arrangement when combinations of two tris-imine ligands react with Fe(II), opening a vast range of possibilities for the synthesis of compounds with interest in spin crossover research. This tendency not always coincides with the solution behaviour, as unveiled by means of mass spectrometry experiments and DFT calculations. Some of the compounds obtained exhibit ordered solvent extrusion processes in a single-crytal-to-single crystal manner, also undergoing a spin switch.